

Natural convection in porous medium-fluid interface problems

Porous medium-fluid interface problems

A finite element analysis by using the CBS procedure

473

Received January 2001
Accepted March 2001

N. Massarotti

*Dipartimento di Meccanica, Strutture, Ambiente e Territorio (DiMSAT),
Università degli Studi di Cassino, Cassino, Italia*

P. Nithiarasu and O.C. Zienkiewicz

*Institute for Numerical Methods in Engineering, University of Wales
Swansea, Swansea, UK*

Keywords Porous medium, Algorithms, Finite elements

Abstract Natural convection in porous medium-fluid interface problems are numerically studied by using the characteristic based split (CBS) algorithm. The finite element method is used to solve the governing generalized porous medium equations. The accuracy of the scheme is estimated by comparing the present predictions for a porous cavity with those results available for the same problem. Two different types of interface problems have been considered. In the first case, the domain is vertically divided into two equal parts, while in the second problem the division is along the horizontal direction. Results obtained from the present investigation are compared extensively with existing experimental and numerical data and they are in good agreement with the available literature. Also present results are smooth along the interface and are without any jumps in the solution.

1. Introduction

The interface between free fluid and a porous medium saturated with the same free fluid is very important in many industrial and real-life applications. Alloy solidification, heat exchanger pipes, petroleum recovery, heat recovery systems, as well as thermal insulation and ground water pollution, are just a few to mention. In these problems the domain can be of the type partly filled with a saturated porous medium and the rest with a free fluid. Although some studies have been reported in the literature, still many issues related to the interface problem have not been adequately addressed. In this paper in addition to a detailed discussion of implementation of the CBS procedure for the porous medium problem, the use of the generalised transient governing equation for interface problems is also explained. Many examples are presented in order to estimate the accuracy of the present procedure. The characteristic-based-split (CBS) procedure is a unified approach for computational fluid dynamics applications. This algorithm was used to solve many problems of fluid dynamics including general compressible and incompressible flow problems (Zienkiewicz and Codina, 1995; Zienkiewicz *et al.*, 1995; Codina *et al.*, 1998;

Nithiarasu and Zienkiewicz, 1999; Zienkiewicz and Nithiarasu, 2000), shallow water (Zienkiewicz and Ortiz, 1995), thermal (Massarotti *et al.*, 1998) and turbulent flows (Zienkiewicz *et al.*, 1995). The CBS has also been used in problems of solid dynamics (Zienkiewicz *et al.*, 1999).

The CBS procedure is developed from the principles of characteristics; in this procedure a particle is tracked along its characteristic (Adey and Brebbia, 1974). A simplified form which includes backward integration is used in the CBS procedure (Löhner *et al.*, 1984). Such a simplification avoids the need for mesh adaptation. In this paper the CBS procedure is implemented to solve applications of porous medium flows. The generalised porous medium equations used in this study are similar to those of incompressible single phase fluids. Therefore, the extension of the CBS to porous medium applications is simple. However, the type of time stepping needs a proper selection. Fully explicit forms are not suitable as an artificial compressibility form for incompressible flows can take an enormous amount of CPU time. Also recovering the transient solution is difficult. Semi-implicit form is suitable, however a straight forward extension of incompressible single phase flow solution procedure is not sufficient (Nithiarasu and Ravindran (1998)). A quasi-implicit form is certainly possible and used in many of our earlier studies (Nithiarasu *et al.*, 1996, 1997a, 1997b, 1997c, 1998, 1999). However, quasi-implicit form needs simultaneous solution at all steps. In this study a semi-implicit form has been employed to save memory and CPU time.

Many studies have been reported on the numerical solution of porous medium equations. Kaviany (1991) and Nield and Bejan (1992) give an excellent summary of flow, heat and mass transfer in a porous medium. Many of the reported works use either finite difference or finite volume procedures to obtain numerical solution to porous medium problems. Also, the application of the generalised porous medium governing equation is not well explored in these studies. Our recent studies by using finite element and the generalised porous medium equations are successful and give accurate results (Nithiarasu and Ravindran, 1998; Nithiarasu *et al.*, 1997a, 1997b, 1997c; Massarotti *et al.*, 2000). In order to further extend these advantages, natural convection in porous-fluid interface problems are considered in this paper.

Although several studies have been reported in the literature on natural convection in fluid saturated porous medium, numerical investigations on partially filled domains with a porous medium-fluid interface are limited (Beckermann *et al.*, 1987; Gartling *et al.*, 1996; Sathe *et al.*, 1988; Alazmi and Vafai, 2001). Although very recently, Alazmi and Vafai (2001) used the generalized model, the problems considered by them are of forced convection type. Applications of most of the other studies are restricted by either Darcy's law or its extensions to porous medium flows. Thus a general procedure addressing all the essential features is necessary in order to understand thoroughly the natural convection in interface problems. In the authors' view, combination of the generalised porous medium equations and the CBS algorithm with finite elements is a good option available to study the interface

problems. In this paper the implementation details of the CBS procedure is presented. In addition to the implementation aspects, some further details on the interface conditions are also discussed in this paper. The paper is organised into the following sections: in the next section, the generalized governing porous medium equations are summarised; the CBS procedure, temporal and spatial discretization are discussed in section 3; in section 4, the interface boundary conditions are presented; some examples including validation of the procedure are given in section 5. Finally, in section 6 some conclusions are drawn from the study carried out.

2. Governing equations

In the present paper incompressible viscous flow through a porous medium has been mathematically described by using the generalized model. The general form of the equation for a medium of variable porosity can be derived by averaging the Navier-Stokes equations over a representative elementary volume (REV), using the well known volume averaging procedure (Whitaker, 1961; Vafai and Tien, 1981; Hsu and Cheng, 1990). The momentum equation for a fluid saturated porous medium can be written as:

$$\rho \left[\frac{\partial \mathbf{u}}{\partial t} + \nabla \left(\frac{\mathbf{u} \cdot \mathbf{u}}{\epsilon} \right) \right] = -\nabla \epsilon p + \mu_e \nabla^2 \mathbf{u} - \left[\frac{\mu \epsilon \mathbf{u}}{K} + \rho \frac{F \epsilon |\mathbf{u}| \mathbf{u}}{K^{1/2}} \right] + \mathbf{B} \quad (1)$$

where all quantities are represented by their average values in the REV. In the above equation \mathbf{u} is the seepage (Darcy) velocity vector, p is the pore fluid pressure, ρ is the fluid density, μ_e is the effective (or Brinkman) viscosity, F is the so called Forchheimer's coefficient, ϵ the porosity of the medium, and \mathbf{B} represents the body forces acting on the system. The hydrodynamic and thermal dispersions have been neglected for the sake of simplicity and the Ergun's correlation (Ergun, 1952), for packed beds, is used to represent the total drag force of the solid matrix on the fluid. In particular the permeability K and the Forchheimer's coefficient F can be written as:

$$K = \frac{\epsilon^3 d_p^2}{a(1 - \epsilon)^2} \quad F = \frac{b}{\sqrt{a} \epsilon^3}$$

with a and b being Ergun's constants, and d_p the average particle size of the bed.

In order to evaluate velocity and temperature fields in the porous medium it is necessary to solve the continuity, momentum and energy equations. For a medium of constant uniform porosity and constant properties except density, the system of equations, (nondimensionalized with respect to the fluid properties) can be written as:

continuity equation:

$$\nabla \cdot \mathbf{u} = 0 \quad (2)$$

momentum equation:

$$\frac{1}{\epsilon} \frac{\partial \mathbf{u}}{\partial t} = -\frac{1}{\epsilon^2} \mathbf{u} \cdot \nabla \mathbf{u} - \nabla p + \frac{R_v Pr}{\epsilon} \nabla^2 \mathbf{u} - \left(\frac{Pr}{Da} + \frac{C}{\sqrt{Da}} |\mathbf{u}| \right) \mathbf{u} + Ra Pr T \mathbf{g} \quad (3)$$

energy equation:

$$R_c \frac{\partial T}{\partial t} = -\mathbf{u} \cdot \nabla T + R_k \nabla^2 T \quad (4)$$

defined in $\Omega \times [0, t]$ with $\Omega \subset \mathbb{R}^2$ domain of interest. In the momentum equations, as mentioned, all the properties are assumed to be constant except fluid density. Fluid density variation is incorporated by invoking the Boussinesq approximation. R_v is the ratio between the effective viscosity and the fluid viscosity, \mathbf{g} the unit vector along the gravity direction, and $C = 1.75/\sqrt{150}$.

In the energy equation T is the temperature, R_k represents the ratio between the conductivity of the fluid and that of the porous medium saturated by stagnant fluid (effective conductivity), and R_c is the nondimensional average volumetric heat capacity ratio, which has been assumed to be constant. The following scales have been employed to nondimensionalise the equations:

$$\mathbf{x} = \frac{\mathbf{x}^*}{L}, \quad \mathbf{u} = \frac{\mathbf{u}^*}{\alpha/L}, \quad p = \frac{p^*}{\rho \alpha^2 / L^2}, \quad t = \frac{t^*}{L^2 / \alpha}, \quad T = \frac{T^* - T_c}{T_h - T_c} \quad (5)$$

and the following nondimensional parameters have been used:

$$Pr = \frac{\mu}{\rho \alpha}, \quad Ra = \frac{g \beta (T_h - T_c) L^3}{\nu \alpha}, \quad Da = \frac{K}{L^2} \quad (6)$$

with α thermal diffusivity, β coefficient of thermal expansion, and μ and ν dynamic and kinematic viscosity of the fluid respectively; \mathbf{x} is the position vector and g represents the magnitude of the gravitational vector, T_h , T_c and L are respectively the hot and cold wall temperatures and the characteristic length of the problem considered. In the above quantities, asterisk is used for dimensional variables. The parameters introduced above are the Raleigh number Ra , the Prandtl number, Pr and the Darcy number, Da .

3. The CBS procedure

As mentioned in the introduction, the CBS (characteristic based split) algorithm, introduced by Zienkiewicz and co-workers for the solution of Navier-Stokes equations, has been adopted to solve the set of generalized porous medium equations. In this section, the CBS procedure for the solution of porous medium equations is described. For more fluid dynamics problems, the reader may refer to other works, mentioned in the introduction.

3.1 Temporal discretization

The momentum equation introduced in the generalized model is similar to convection-diffusion equation and can therefore be discretized in time using the characteristic-Galerkin process. In particular, the time discrete momentum equation in its semi-implicit form can be written as

$$\begin{aligned} \frac{u_i^{n+1} - u_i^n}{\epsilon \Delta t} &= \left[-\frac{u_j \partial u_i}{\epsilon^2 \partial x_j} + \frac{R_v Pr}{\epsilon} \frac{\partial^2 u_i}{\partial x_j \partial x_j} + \frac{\Delta t}{2} u_k \frac{\partial}{\partial x_k} \left(\frac{u_j \partial u_i}{\epsilon^2 \partial x_j} \right) \right]^n + \\ &- \theta_1 \left[\frac{Pr}{Da} u_i + C \frac{|\mathbf{u}|}{\sqrt{Da} \epsilon^{3/2}} u_i \right]^{n+1} - (1 - \theta_1) \left[\frac{Pr}{Da} u_i + C \frac{|\mathbf{u}|}{\sqrt{Da} \epsilon^{3/2}} u_i \right]^n + Ra Pr T^n g_i \\ &- \theta_2 \left[\frac{\partial p}{\partial x_i} \right]^{n+1} - (1 - \theta_2) \left[\frac{\partial p}{\partial x_i} - \frac{\Delta t}{2} u_k \frac{\partial \partial p}{\partial k \partial x_i} \right]^n \end{aligned} \quad (7)$$

In the above equation $\theta_1 = 1$ and $\theta_2 = 1$ have been employed in this paper. The pressure in the equation has to be treated as a known quantity and therefore needs to be computed from another equation. Although researchers have used quasi-implicit techniques to solve these porous medium equations (Nithiarasu *et al.*, 1996, 1997a, 1997b, 1997c, 1998, 1999) in the present work a semi-implicit procedure, of the type introduced by Nithiarasu and Ravindran (1998), is used. Taking all terms due to the porous matrix to the left hand side of the equation, we have

$$\begin{aligned} \frac{u_i^{n+1}}{\epsilon \Delta t} + \frac{Pr}{Da} u_i^{n+1} + C \frac{|\mathbf{u}|}{\sqrt{Da} \epsilon^{3/2}} u_i^{n+1} &= \frac{u_i^n}{\epsilon \Delta t} - \left[\frac{\partial p}{\partial x_i} \right]^{n+1} - \left[\frac{u_j \partial u_i}{\epsilon^2 \partial x_j} \right]^n + \\ &+ \left[\frac{\Delta t}{2} u_k \frac{\partial}{\partial x_k} \left(\frac{u_j \partial u_i}{\epsilon^2 \partial x_j} \right) \right]^n + \left[\frac{R_v Pr}{\epsilon} \frac{\partial^2 u_i}{\partial x_j \partial x_j} \right]^n + Ra Pr T^n g_i \end{aligned} \quad (8)$$

The first step of the CBS algorithm is the calculation of an intermediate velocity $\tilde{\mathbf{u}}$ from the momentum equation without including the pressure terms. We now have

$$\begin{aligned} \left(\frac{1}{\epsilon \Delta t} + \frac{Pr}{Da} + C \frac{|\mathbf{u}|}{\sqrt{Da} \epsilon^{3/2}} \right) \tilde{u}_i &= \frac{u_i^n}{\epsilon \Delta t} - \left[\frac{u_j \partial u_i}{\epsilon^2 \partial x_j} \right]^n + \\ &+ \left[\frac{\Delta t}{2} u_k \frac{\partial}{\partial x_k} \left(\frac{u_j \partial u_i}{\epsilon^2 \partial x_j} \right) \right]^n + \left[\frac{R_v Pr}{\epsilon} \frac{\partial^2 u_i}{\partial x_j \partial x_j} \right]^n + Ra Pr T^n g_i \end{aligned} \quad (9)$$

In the second step the pressure is calculated from a modified Poisson equation, which ensures the continuity equation to be satisfied, and for the generalized model can be written as:

$$\left[\frac{\partial^2 p}{\partial x_i \partial x_i} \right]^{n+1} = \left(\frac{1}{\epsilon \Delta t} + \frac{Pr}{Da} + C \frac{|\mathbf{u}|}{\sqrt{Da} \epsilon^{3/2}} \right) \cdot \left[\frac{\partial \tilde{u}_i}{\partial x_i} \right] \quad (10)$$

In the third step the real velocity values are obtained from the following correction, obtained simply by subtracting equation (9) from equation (8):

$$u_i^{n+1} = \tilde{u}_i - \left(\frac{1}{\epsilon \Delta t} + \frac{Pr}{Da} + C \frac{|\mathbf{u}|}{\sqrt{Da} \epsilon^{3/2}} \right)^{-1} \cdot \left[\frac{\partial p}{\partial x_i} \right]^{n+1} \quad (11)$$

For thermal flow problems, the next step of the procedure involves the time discretization of the energy equation, in which the velocities are known from the previous steps.

$$T^{n+1} = T^n - \frac{\Delta t}{R_c} \left[u_j \frac{\partial T}{\partial x_j} - R_k \frac{\partial^2 T}{\partial x_j \partial x_j} - \frac{\Delta t}{2} u_k \frac{\partial}{\partial x_k} \left(u_j \frac{\partial T}{\partial x_j} \right) \right]^n \quad (12)$$

Once the equations have been discretized in space it is possible to solve them in the order presented, so evaluating all the variables at time $n + 1$.

At this stage the above system of equations can be discretized in space as described below.

3.2 Spatial discretization and solution procedure

When the characteristic-Galerkin procedure is used, the Galerkin spatial approximation is justified. The weak form of the above system of equations, using the standard Galerkin approximation, can be written as

Step 1: intermediate velocity calculation

$$\begin{aligned} \int_{\Omega} N^k \left(\frac{1}{\epsilon \Delta t} + \frac{Pr}{Da} + C \frac{|\mathbf{u}|}{\sqrt{Da} \epsilon^{3/2}} \right) \tilde{u}_i d\Omega &= \left[\int_{\Omega} N^k \left(\frac{u_i}{\epsilon \Delta t} \right) d\Omega \right]^n \\ &- \left[\int_{\Omega} N^k \left(\frac{u_j}{\epsilon^2} \frac{\partial u_i}{\partial x_j} \right) d\Omega \right]^n + \frac{\Delta t}{2} \left[\int_{\Omega} N^k \left(u_k \frac{\partial}{\partial x_k} \left(\frac{u_j}{\epsilon} \frac{\partial u_i}{\partial x_j} \right) \right) d\Omega \right]^n \\ &+ \left[\frac{R_v Pr}{\epsilon} \int_{\Omega} N^k \left(\frac{\partial^2 u_i}{\partial x_j \partial x_j} \right) d\Omega \right]^n + \left[Ra Pr \int_{\Omega} N^k (T g_i) d\Omega \right]^n \end{aligned} \quad (13)$$

Step 2: pressure calculation

$$\begin{aligned} \left[\int_{\Omega} N^k \left(\frac{\partial^2 p}{\partial x_i \partial x_i} \right) d\Omega \right]^{n+1} &= \\ \left(\frac{1}{\epsilon \Delta t} + \frac{Pr}{Da} + \frac{1.75}{\sqrt{150}} \frac{|\mathbf{V}|}{\sqrt{Da} \epsilon^{3/2}} \right) \cdot \left[\int_{\Omega} N^k \left(\frac{\tilde{u}_i}{\partial x_i} \right) d\Omega \right] \end{aligned} \quad (14)$$

Step 3: velocity correction

$$\int_{\Omega} N^k(u_i)^{n+1} d\Omega = \int_{\Omega} N^k(\tilde{u}_i) d\Omega - \left(\frac{1}{\epsilon \Delta t} + \frac{Pr}{Da} + \frac{1.75}{\sqrt{150}} \frac{|\mathbf{V}|}{\sqrt{Da}} \frac{1}{\epsilon^{3/2}} \right)^{-1} \cdot \left[\int_{\Omega} N^k \left(\frac{\partial p}{\partial x_i} \right) d\Omega \right]^{n+1} \quad (15)$$

Step 4: Temperature calculation

$$\frac{R_c}{\Delta t} \int_{\Omega} N^k(T)^{n+1} d\Omega = \frac{R_c}{\Delta t} \int_{\Omega} N^k(T)^n d\Omega - \left[\int_{\Omega} N^k \left(u_j \frac{\partial T}{\partial x_j} \right) d\Omega - \int_{\Omega} N^k \left(R_k \frac{\partial^2 T}{\partial x_j \partial x_j} \right) d\Omega \right]^n \quad (16)$$

$$+ \left[\frac{\Delta t}{2} \int_{\Omega} N^k \left(u_k \frac{\partial}{\partial x_k} \left(u_j \frac{\partial T}{\partial x_j} \right) \right) d\Omega \right]^n \quad (17)$$

In this work equal order interpolation functions have been used for velocities, pressure, and temperature. Therefore the variables have been approximated as follows:

$$\mathbf{u}_i = \mathbf{N} \mathbf{u}_i \quad \tilde{\mathbf{u}}_i = \mathbf{N} \tilde{\mathbf{u}}_i \quad p = \mathbf{N} \mathbf{p} \quad T = \mathbf{N} \mathbf{T} \quad (18)$$

where the shape functions $\mathbf{N} = [N^1 \dots N^k \dots N^m]$ are the weighting functions as we are using the standard Galerkin procedure, and the nodal values of the variables are:

$$\mathbf{u}_i = [u_i^1 \dots u_i^k \dots u_i^m]^T \quad \tilde{\mathbf{u}}_i = [\tilde{u}_i^1 \dots \tilde{u}_i^k \dots \tilde{u}_i^m]^T$$

$$\mathbf{p} = [p^1 \dots p^k \dots p^m]^T \quad \mathbf{T} = [T^1 \dots T^k \dots T^m]^T$$

Introducing the approximated functions (18) in equations (13)-(16) we finally have the following system of algebraic equations, written in matrix form:

Step 1:

$$POR [\mathbf{M}] \{ \tilde{\mathbf{u}}_i \} = \frac{1}{\epsilon} [\mathbf{M}] \{ \mathbf{u}_i \}^n + -\frac{\Delta t}{\epsilon^2} [\mathbf{C}] \{ \mathbf{u}_i \}^n + \Delta t \frac{R_v Pr}{\epsilon} ([\mathbf{K}] \{ \mathbf{u}_i \}^n + \{ \mathbf{f}_u \}^n) + \left(\frac{\Delta t}{\epsilon} \right)^2 [\mathbf{K}_u] \{ \mathbf{u}_i \}^n + \Delta t Ra Pr [\mathbf{M}] \{ \mathbf{T} \}^n g_i \quad (19)$$

Step 2:

$$[\mathbf{K}] \{ \mathbf{p} \}^{n+1} = \frac{POR}{\Delta t} [\mathbf{Q}] \{ \tilde{\mathbf{u}}_i \} \quad (20)$$

Step 3:

$$[\mathbf{M}] \{\mathbf{u}\}^{n+1} = [\mathbf{M}] \{\tilde{\mathbf{u}}_i\} - \frac{\Delta t}{POR} [\mathbf{Q}] \{\mathbf{p}\}^{n+1} \quad (21)$$

Step 4:

$$\begin{aligned} [\mathbf{M}] \{\mathbf{T}\}^{n+1} &= [\mathbf{M}] \{\mathbf{T}\}^n - \frac{\Delta t}{R_c} [\mathbf{C}] \{\mathbf{T}\}^n \\ &+ \Delta t \frac{R_k}{R_c} ([\mathbf{K}] \{\mathbf{T}\}^n + \{\mathbf{f}_T\}^n) + \frac{\Delta t^2}{R_c} [\mathbf{K}_u] \{\mathbf{T}\}^n \end{aligned} \quad (22)$$

where:

$$\begin{aligned} [\mathbf{M}] &= \int_{\Omega} \mathbf{N}^T \mathbf{N} d\Omega & [\mathbf{C}] &= \int_{\Omega} \mathbf{N}^T \mathbf{u}_i \frac{\partial \mathbf{N}}{\partial x_i} d\Omega & \{\mathbf{f}_u\}^n &= \int_{\Gamma} \mathbf{N}^T \mathbf{n}^T \frac{\partial \mathbf{u}}{\partial x_i} d\Gamma \\ [\mathbf{K}] &= \int_{\Omega} \frac{\partial \mathbf{N}^T}{\partial x_i} \frac{\partial \mathbf{N}}{\partial x_i} d\Omega & [\mathbf{Q}] &= \int_{\Omega} \mathbf{N}^T \frac{\partial \mathbf{N}}{\partial x_i} d\Omega & \{\mathbf{f}_T\}^n &= \int_{\Gamma} \mathbf{N}^T \mathbf{n}^T \frac{\partial \mathbf{T}}{\partial x_i} d\Gamma \\ [\mathbf{K}_u] &= -\frac{1}{2} \int_{\Omega} \mathbf{N}^T \mathbf{N} u_i \frac{\partial \mathbf{N}^T}{\partial x_i} d\Omega \end{aligned}$$

and

$$POR = \frac{1}{\epsilon} + \Delta t \frac{Pr}{Da} + \Delta t C \frac{|\mathbf{u}|}{\sqrt{Da} \epsilon^{3/2}}$$

In the above discretized equations second order terms have been integrated by parts and vectors $\{\mathbf{f}\}$ represent the related boundary integrals. Boundary terms that result from integration by parts of the stabilizing terms are not included as they have no influence on the solution. Equations (15)-(18) can be used for the solution of incompressible natural convective flow through a porous medium and for single phase natural convective flows with appropriate changes in the porosity values. As mentioned before, changing the properties such as porosity and thus permeability, it is possible to handle porous-free fluid interface problems as a single problem with different properties. The following porosity limits are used for a porous medium part and single-phase fluid part.

$$\begin{aligned} \epsilon < 1 & \Rightarrow \text{porous medium} & \epsilon = 1 & \Rightarrow \text{free fluid} \\ Da = \text{finite} & & Da \rightarrow \infty & \end{aligned} \quad (23)$$

We just need a suitable set of matching conditions to connect the porous and single-phase domains. In the following section, the interface conditions are discussed for a porous-fluid interface problem.

4. Interface matching conditions

Matching conditions for velocity, pressure and temperature at the interface between a porous layer and a free fluid are still not well established. Although mass, momentum and energy conservation is clearly satisfied across the interface in the microscopic approach, it is not clear at the macroscopic level (Gartling *et al.*, 1996; Alazmi and Vafai, 2001). In the present work, no attempt has been made to establish any new conditions across the boundary and the classical continuity conditions have been employed. When continuity of mass, momentum and energy is assumed, the following matching conditions need to be satisfied at the interface:

$$\begin{aligned} (u_i^f - u_i^p)n_i &= 0 \\ (\sigma_{ij}^f - \sigma_{ij}^p)n_j &= 0 \\ (\tau_{ij}^f - \tau_{ij}^p)t_j &= 0 \end{aligned} \quad (24)$$

where superscripts *f* and *p* refer respectively to free fluid and porous medium; n_i is the unit vector normal to the interface and t_j is the unit vector in tangential direction; τ_{ij} is the deviatoric or viscous stress, and σ_{ij} is the tangential stress.

The above conservation equation, using the standard Newtonian constitutive relations for the tangential stress, do not provide any constraints on the tangential component of the velocity. This assumption was explicitly made in the present work. Pressure is generally assumed to be continuous across the interface and this requires that the normal components of the fluid viscous stress are balanced across the interface (Gartling *et al.*, 1996). Nield and Bejan (1992) argued that in this way the stress in the solid matrix is not taken into account properly. The authors are aware of the fact that this will lead to an over prediction of the flow magnitude and influx into the porous medium. However, this short coming may be overcome through a better understanding of the Brinkman viscosity, but for the sake of simplicity, in this paper the effective viscosity is assumed equal to the fluid viscosity. Further study on the calculation of equivalent viscosity is being carried out in order to get a better approximation of interface conditions. In addition to conditions mentioned above, continuity of tangential velocity is also imposed. This assumption is valid at least for the nodes where the porosity is close to unity. Further research is being carried out by the authors to validate this assumption. With regards to thermal conditions, local thermal equilibrium and the energy conservation are assumed along the interface:

$$\begin{aligned} T^f - T^p &= 0 \\ \left(\frac{\partial T^f}{\partial x_i} - R_k \frac{\partial T^p}{\partial x_i} \right) n_i &= 0 \end{aligned} \quad (25)$$

With the above assumptions, the nodal equations (19)-(22) do not need any particular treatment at the interface. The nodes placed along the interface will

HFF
11,5

get adequate contributions from elements placed in the fluid and in the porous medium.

5. Results

In this section, the numerical results are presented. In the following subsection the present procedure is validated by using some bench-mark porous medium problems. In a later subsection two types of interface problems are discussed in detail.

482

5.1 Natural convection in a square cavity filled with fluid saturated porous medium

The accuracy of the present solution methodology is verified by solving the natural convective flow in a differentially heated square cavity filled with fluid saturated porous medium. The no slip boundary conditions are assumed on all walls. The horizontal walls are assumed to be insulated. The mesh used for this case has 2,601 nodes and 5,000 elements. The mesh is non-uniform and a geometric progression is used to generate a finer mesh near the walls and coarser towards the center. The first nodal point is placed at a non-dimensional distance of 0.005 from the walls.

In Tables I and II, the results obtained from the present computations are compared with the available analytical and numerical results. As seen the results obtained by the CBS procedure is in good agreement with available data for the Darcy and Rayleigh number range considered.

5.2 Porous-free fluid interface problems

Two types of interface problems have been considered to test the present CBS procedure. In the first case, the domain is divided vertically into two equal parts and one part is filled with a free fluid and the other with a porous medium

Da	10^{-6}	10^{-4}	10^{-2}					
Ra	10^7	10^8	10^9	10^6	10^3	10^4	10^5	Reference
	1.074	2.969	11.699	2.580	1.008	1.359	2.986	Nithiarasan and Ravindran (1998)
	1.079	2.970	11.460	2.550	1.010	1.408	2.983	Nithiarasan <i>et al.</i> (1997a,b,c)
	1.072	3.039	13.464	2.722	1.001	1.404	3.110	Present

Table I.
Comparison of the average Nusselt number

Ra	10^7	10^8	10^9	Reference
	1.074	2.99	12.30	Nithiarasu and Ravindran (1998)
	-	3.09	12.49	Walker and Hosmy (1978)
	1.07	3.09	13.41	Lauriat and Prasad (1989)
	-	3.27	18.38	Trevisan and Bejan (1985)
	1.080	3.02	12.51	Nithiarasu <i>et al.</i> (1996)
	1.072	3.04	13.46	Present

Table II.
Average Nusselt number for the Darcy regime, $Da = 10^{-6}$

saturated by the same fluid. The vertical wall adjacent to the free fluid, on the left hand side of the cavity, is considered to be hot, while the opposite wall, adjacent to the porous matrix, is cold. In the second case considered, the domain is equally divided into two parts horizontally and the bottom portion is assumed to be filled with the fluid saturated porous medium. Figure 1 shows the finite element mesh and boundary conditions for the first problem. The mesh is graded near all walls and along the interface of the problem which is at the middle of the cavity. The domain is meshed with 4,608 elements and 2,401 nodes.

The stream lines and isotherm patterns obtained for the vertical interface problem are shown in Figure 2 for the Darcy regime ($Ra = 3.028 \times 10^7$, $Da = 7.354 \times 10^{-7}$, $Pr = 6.97$, $\epsilon = 0.36$, $R_k = 1.397$). As seen, the results

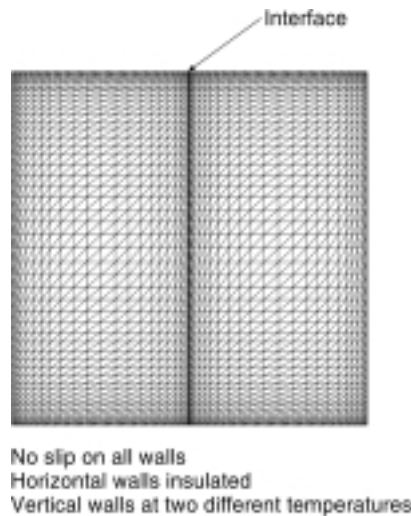


Figure 1. Natural convective flow in a porous-free fluid vertical interface problem. Finite element mesh and boundary conditions

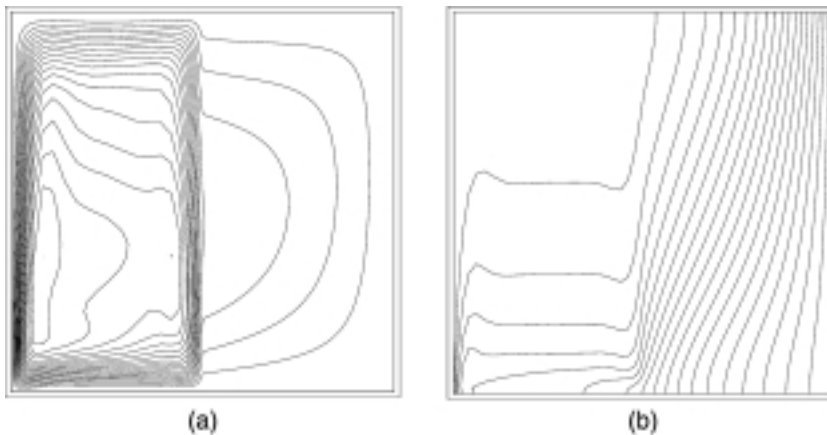


Figure 2. Natural convective flow in a porous-free fluid, vertical interface problem: Darcy regime (a) Stream lines; (b) isotherms

obtained with the CBS procedure predict the interface transition smoothly without any form of jump. Since this figure corresponds to the Darcy regime, the porous medium part (right half) is dominated mainly by conduction mode of heat transfer. The flow in the porous medium part is weaker than that in the free fluid region. A maximum stream function value of $|\Psi|_{\max}=15.38$ is observed in the fluid region and the value obtained by Beckermann *et al.* (1987) is $|\Psi|_{\max}=15.98$. The flow and isotherm patterns presented here are in excellent agreement with the experiments and numerical results of Beckermann *et al.* (1987). Figure 3 shows the comparison of temperature distribution at different horizontal sections across the cavity with experimental and available numerical data. The agreement is excellent, and in particular it can be noticed that the change in slope of the isotherms at the interface is well predicted. Furthermore there seems to be an over prediction of the fluid penetration into the porous region. This result, as previously mentioned was expected and could be improved using a proper value for the effective viscosity.

In Figure 4, the results obtained in the non-Darcy regime ($Ra = 3.028 \times 10^7$, $Da = 1.296 \times 10^{-5}$, $Pr = 6.97$, $\epsilon = 0.38$, $R_k = 1.383$) have been given. As expected the fluid influx into the porous medium is much higher than that of the Darcy flow regime of Figure 2. However, the flow in the porous region is not as strong as it is in the free fluid. The thermal boundary layer near the top right

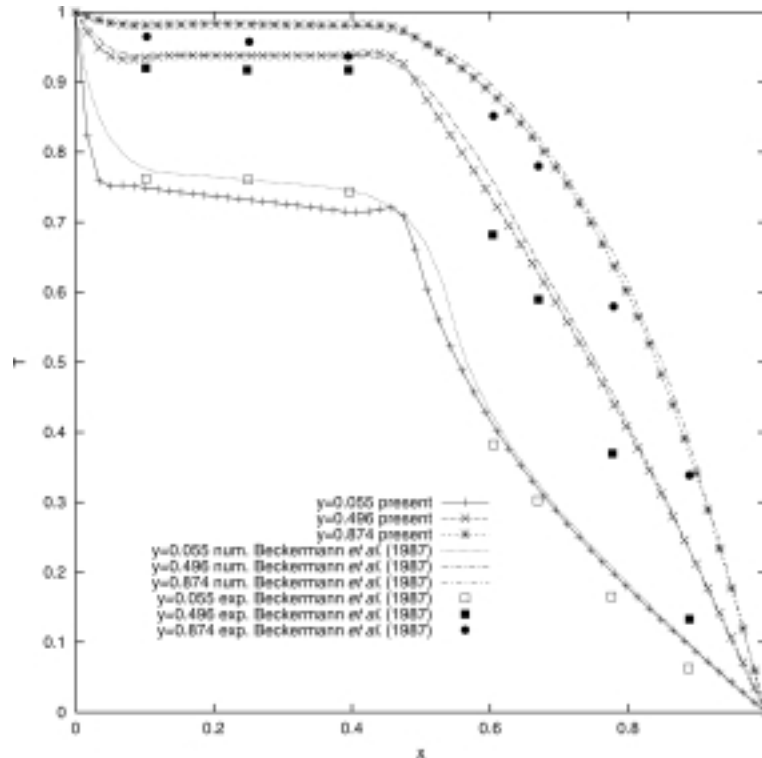


Figure 3.
Natural convective flow
in a porous-free fluid
vertical interface
problem Darcy regime.
Comparison of
temperature distribution
with experiments

corner in the porous region is observed to be thicker than that of the bottom left corner in the fluid region. However, towards the bottom the boundary layer expands slowly in the porous region but towards the top, in the fluid region the expansion of the boundary layer is rapid with almost zero heat flux at the top left corner. This is the way in which the energy is conserved in these porous-free fluid interface problems.

As mentioned earlier, the second type of problem is an enclosure divided horizontally as shown in Figure 5(a). The bottom half-filled with the fluid

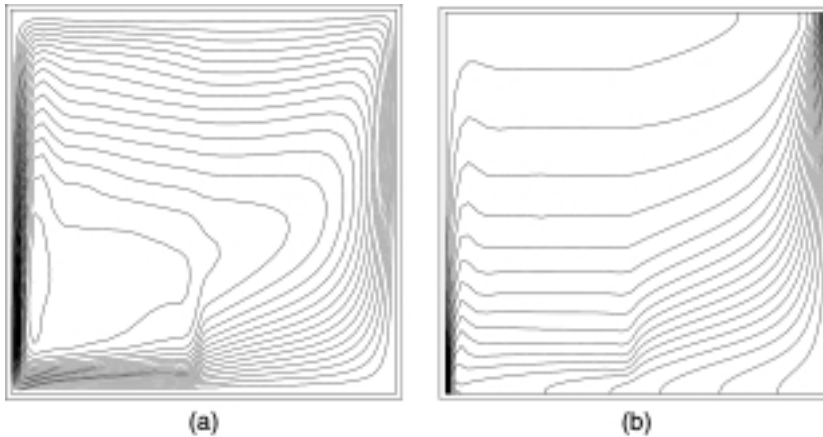


Figure 4. Natural convection flow in porous-free fluid vertical interface problem non-Darcy regime: (a) stream lines; (b) isotherms

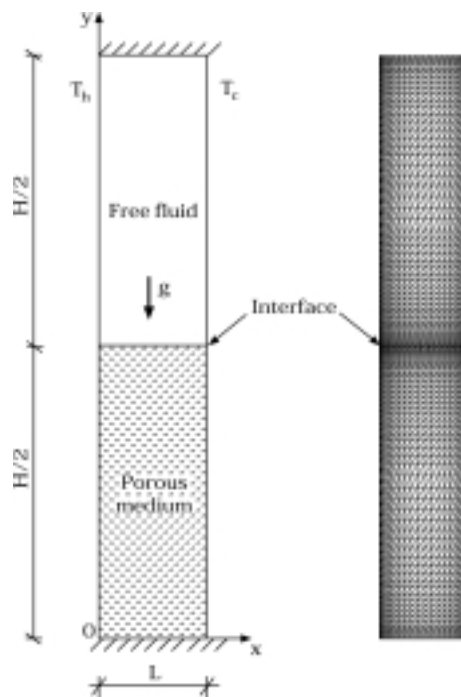


Figure 5. Natural convective flow in a porous-free fluid horizontal interface problem: (a) geometry, thermal boundary conditions and (b) mesh used

saturated porous matrix. The mesh generated for this problem contains 2,231 points and 4,224 elements, which are not homogeneously distributed, as shown in Figure 5(b). All the walls are assumed to obey no slip conditions, horizontal walls are insulated and vertical walls are placed at two different temperatures which trigger the buoyant flow.

Figures 6(a) and (b) show respectively the stream lines and isotherms for the horizontally divided problem calculated by using: $Ra = 10^5$, $Da = 10^{-3}$, $Pr = 10.0$, $\epsilon = 0.4$, $R_k = 1.0$. As seen the flow is smooth without any jump in the solution. As expected the flow in the fluid region is much stronger than that of the porous region. The heat transport across the cavity is much higher in the fluid region than that of the porous region as the convection is stronger there.

In order to compare the results obtained using the present CBS procedure with some experiments, one case for high a Prandtl number was run, and the results are compared in Figure 7 with those presented by Nishimura *et al.*

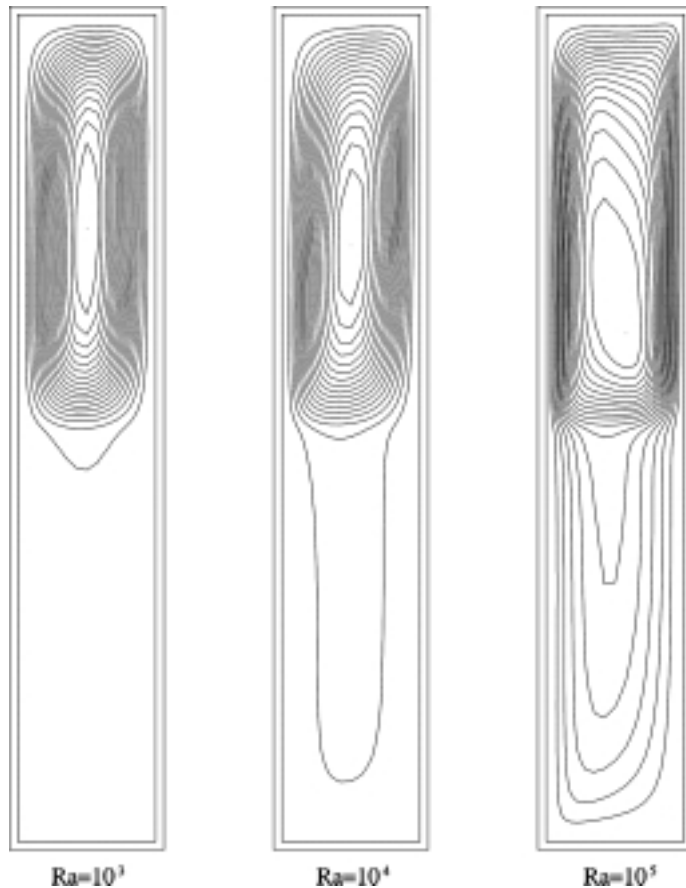


Figure 6(a).
Natural convective flow
in a porous-free fluid
horizontal interface
problem, stream lines at
different Rayleigh
numbers, $Da = 10^{-3}$,
 $Pr = 10$, $R_k = 1.0$

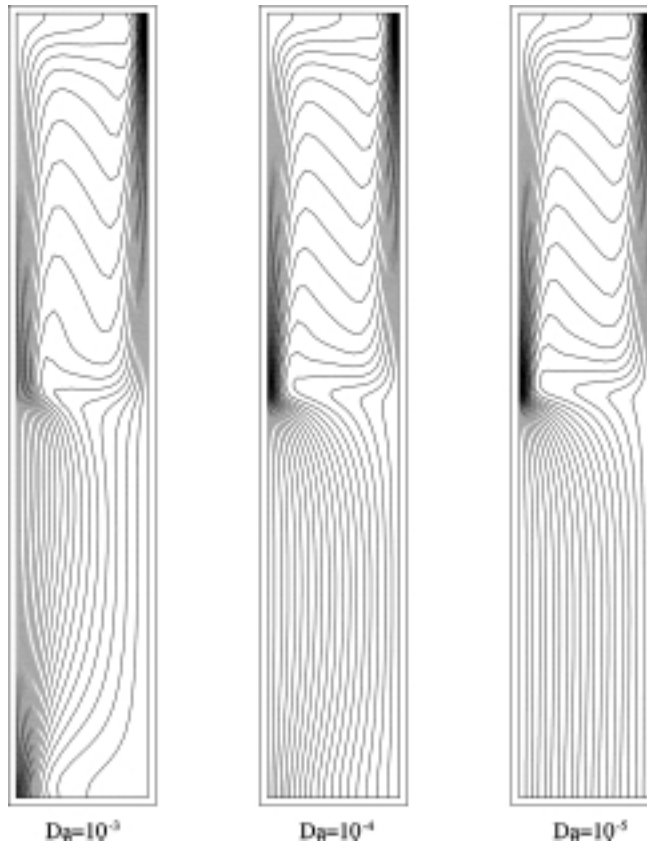


Figure 6(b).
Natural convective flow
in porous-free fluid
horizontal interface
problem, isotherms at
different Darcy
numbers, $Ra = 10^5$,
 $Pr = 10$, $R_k = 1.0$

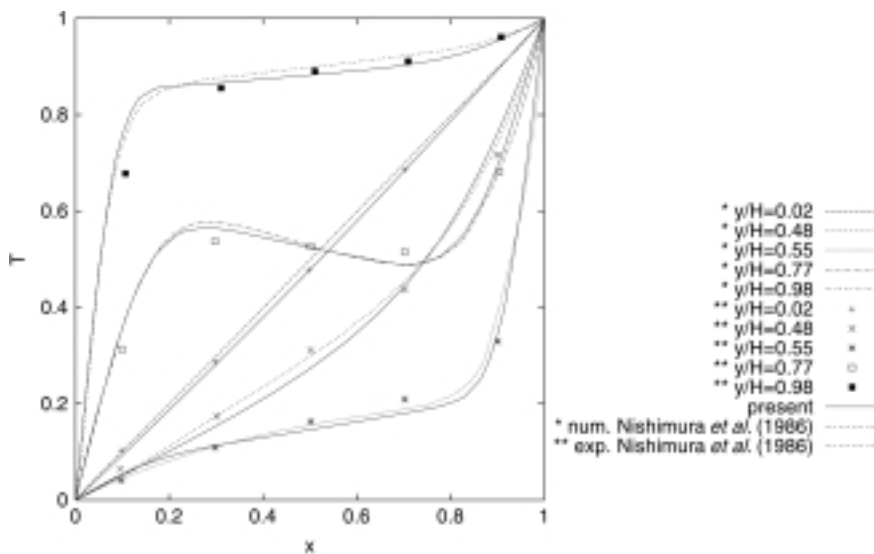


Figure 7.
Natural convective flow
in a porous-free fluid
horizontal interface
problem, temperature
distribution for
 $Da = 3.5 \times 10^{-6}$,
 $Ra = 10^5$, $Pr = 8,000$,
 $R_k = 1.0$

(1986) for silicon oil as the fluid and glass beads as the solid matrix. The temperature is evaluated at five different horizontal sections, in the porous as well as in the fluid part of the cavity. The present results, in general, are in excellent agreement with experimental data. In Figure 8 the local Nusselt number on the cold wall at two different Darcy numbers is compared to the other numerical results. It can be noticed that, while in the porous medium the agreement is excellent, in the fluid part there is a small difference, especially on the peak values. The over prediction of Nishimura *et al.* (1986) could be attributed to the coarse mesh and difference in the model employed.

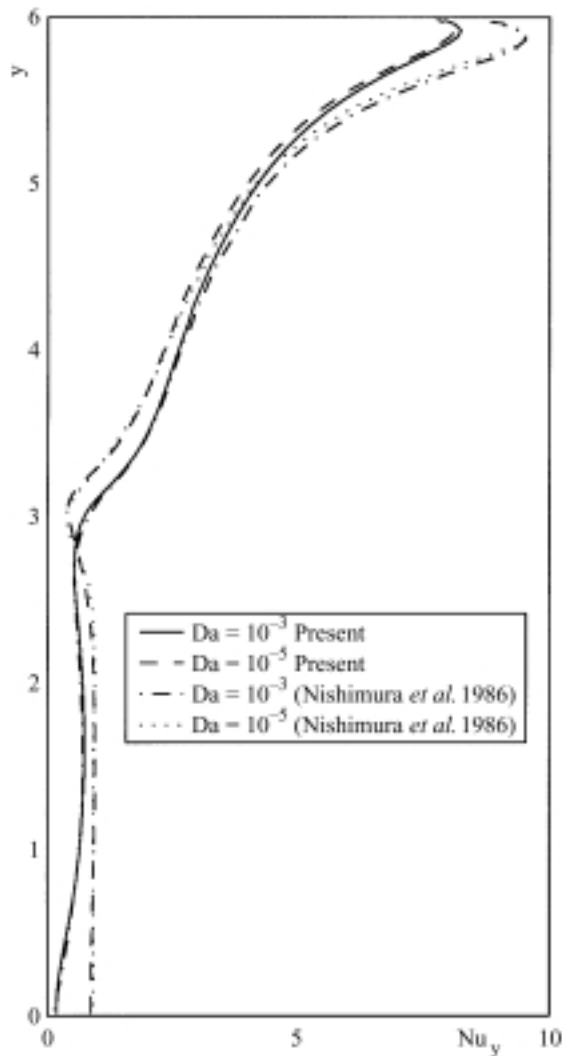


Figure 8. Natural convective flow in a porous-free fluid horizontal interface problem, local Nusselt number distributions, $Ra = 5 \times 10^4$, $Pr = 10$, $R_k = 1.0$

6. Conclusions

In this paper, the characteristic based split (CBS) algorithm was implemented for a porous-free fluid interface problem. The finite element method was successfully employed to solve the governing generalized porous medium equations. It was demonstrated that the generalized porous medium model without any special treatment can be applied to both porous medium and free fluid in a single domain. The results obtained for both the problems considered were in good agreement with the available numerical and experimental data. Further study is necessary to extend the present procedure for more complex geometries.

References

- Adey, A.R. and Brebbia, C.A. (1974), "Finite element solution of effluent dispersion", in Brebbia, C.A. and Connor, J.J. (Eds), *Numerical Methods in Fluid Mechanics*, Pentech Press, London, pp. 325-54.
- Alazmi, B. and Vafai, K. (2001), "Analysis of fluid flow and heat transfer interfacial conditions between a porous medium and a fluid layer", *Int. J. Heat Mass Transfer*, Vol. 44, pp. 1735-49.
- Beckermann, C., Ramadhyani, S. and Viskanta, R. (1987), "Natural convection flow and heat transfer between a fluid layer and a porous layer inside a rectangular enclosure", *ASME J. Heat Transfer*, Vol. 109, pp. 363-70.
- Codina, R., Vázquez, M. and Zienkiewicz, O.C. (1998), "General algorithm for compressible and incompressible flows Part III – a semi-implicit form", *Int. J. Num. Meth. Fluids*, Vol. 27, pp. 13-32.
- Ergun, S. (1952), "Fluid flow through packed column", *Che. Eng. Pro.*, Vol. 48, pp. 89-94.
- Gartling, D.K., Hickox, C.E. and Givler, R.C. (1996), "Simulation of coupled viscous and porous flow problems", *Comp. Fluid Dyn.*, Vol. 7, pp. 23-48.
- Hsu, C.T. and Cheng, P. (1990), "Thermal dispersion in a porous medium", *Int. J. Heat Mass Transfer*, Vol. 33, pp. 1587-97.
- Kaviany, M. (1991), *Principles of Heat Transfer in Porous Media*, Springer-Verlag, New York, NY.
- Lauriat, G. and Prasad, V. (1989), "Non-Darcian effects on natural convection in a vertical porous enclosure", *Int. J. Heat Mass Transfer*, Vol. 32, pp. 2135-48.
- Löhner, R., Morgan, K. and Zienkiewicz, O.C. (1984), "The solution of non-linear hyperbolic equation systems by the finite element method", *Int. J. Num. Meth. Fluids*, Vol. 4, pp. 1043-63.
- Massarotti, N., Nithiarasu, P. and Zienkiewicz, O.C. (1998), "Characteristic-based-split (CBS) algorithm for incompressible flow problems with heat transfer", *Int. J. Num. Meth. Heat Fluid Flow*, Vol. 8, pp. 969-90.
- Massarotti, N., Nithiarasu, P. and Zienkiewicz, O.C. (2000), "Porous-fluid interface problems, a characteristic-based-split (CBS) procedure", *Proceedings of the ECCOMAS 2000*, September 2000, Barcelona.
- Nield, D.A. and Bejan, A. (1992), *Convection in Porous Media*, Springer-Verlag, New York, NY.
- Nishimura, T., Takumi, T., Shiraiishi, M., Kawamura, Y. and Ozoe, H. (1986), "Numerical analysis of natural convection in a rectangular enclosure horizontally divided into fluid and porous regions", *Int. J. Heat Mass Transfer*, Vol. 29, pp. 889-98.

- Nithiarasu, P. and Ravindran, K. (1998), "A new semi-implicit time stepping procedure for buoyancy driven flow in saturated porous medium", *Comp. Methods Appl. Mech. Eng.*, Vol. 165, pp. 147-54.
- Nithiarasu, P. and Zienkiewicz, O.C. (1999), "On stabilization of the CBS algorithm. Internal and external time steps", *Int. J. Num. Meth. Eng.*, Vol. 48, pp. 875-80.
- Nithiarasu, P., Seetharamu, K.N. and Sundararajan, T. (1996), "Double-diffusive natural convection in an enclosure filled with saturated porous medium – a generalised non-Darcy approach", *Numer. Heat Transfer, Part A*, Vol. 30, pp. 413-26.
- Nithiarasu, P., Seetharamu, K.N. and Sundararajan, T. (1997a), "Natural convective heat transfer in an enclosure filled with fluid saturated variable porosity medium", *Int. J. Heat Mass Transfer*, Vol. 40, pp. 3955-67.
- Nithiarasu, P., Seetharamu, K.N. and Sundararajan, T. (1997b), "Non-Darcy double-diffusive convection in fluid saturated axisymmetric porous cavities", *Heat and Mass Transfer*, Vol. 36, pp. 427-34.
- Nithiarasu, P., Seetharamu, K.N. and Sundararajan, T. (1997c), "Double-diffusive natural convection in a fluid saturated porous cavity with a freely convecting wall", *Int. Comm. Heat Mass Transfer*, Vol. 24, pp. 1121-30.
- Nithiarasu, P., Seetharamu, K.N. and Sundararajan, T. (1998), "Effects of porosity on natural convective heat transfer in a fluid saturated porous medium", *Int. J. Heat Fluid Flow*, Vol. 19, pp. 56-8.
- Nithiarasu, P., Seetharamu, K.N. and Sundararajan, T. (1999), "Numerical prediction of buoyancy driven flow in a fluid saturated non-Darcian porous medium", *Int. J. Heat Mass Transfer*, Vol. 42, pp. 1205-15.
- Sathe, S.B., Lin, W.Q. and Tong, T.W. (1988), "Natural convection in an enclosure containing an insulation with a permeable fluid-porous interface", *Int. J. Heat and Fluid Flow*, Vol. 9, pp. 389-95.
- Trevisan, O.V. and Bejan, A. (1985), "Natural convection with combined heat and mass transfer buoyancy effects in a porous medium", *Int. J. Heat Mass Transfer*, Vol. 28, pp. 1597-611.
- Vafai, K. and Tien, C.L. (1981), "Boundary and inertia effects on flow and heat transfer in porous media", *Int. J. Heat Mass Transfer*, Vol. 24, pp. 195-203.
- Walker, K.L. and Hosmy, G.M. (1978), "Convection in porous cavity", *J. Fluid Mech.*, Vol. 87, pp. 449-74.
- Whitaker, S. (1961), "Diffusion and dispersion in porous media", *A.I.Ch.E. J.*, Vol. 13, pp. 420-7.
- Zienkiewicz, O.C. and Codina, R. (1995), "A general algorithm for compressible and incompressible flow, Part I. The split characteristic based scheme", *Int. J. Num. Meth. Fluids*, Vol. 20, pp. 869-85.
- Zienkiewicz, O.C. and Nithiarasu, P. (2000), "An universal algorithm for fluid dynamics. The characteristic based split (CBS) procedure. Some tests on stability and boundary conditions", *Archives of Mechanics*, Vol. 52, pp. 857-87.
- Zienkiewicz, O.C. and Ortiz, P. (1995), "A split-characteristic based finite element model for the shallow water equations", *Int. J. Num. Meth. Fluids*, Vol. 20, pp. 1061-80.
- Zienkiewicz, O.C., Nithiarasu, P., Codina, R., Vázquez, M. and Ortiz, P. (1999), "An efficient and accurate algorithm for fluid mechanics problems. The characteristic based split (CBS) algorithm", *Int. J. Num. Meth. Fluids*, Vol. 31, pp. 359-92.
- Zienkiewicz, O.C., Rojek, J., Taylor, R.L. and Pastor, M. (1999), "Triangles and tetrahedra in explicit dynamics codes for solids", *Int. J. Num. Meth. Eng.*, Vol. 43, pp. 565-83.
- Zienkiewicz, O.C., Satya Sai, B.V.K., Morgan, K., Codina, R. and Vázquez, M. (1995), "A general algorithm for compressible and incompressible flow – Part II. Tests on the explicit form", *Int. J. Num. Meth. Fluids*, Vol. 20, pp. 887-913.